Construction of Low Noise Electrochemical Quartz Crystal Microbalance

Euijin Hwang* and Youngran Lim

Electrochemistry Group, Korea Research Institute of Standards and Science, Taejon 305-340, Korea

Received September 22, 1995

A new oscillator for electrochemical quartz crystal microbalance (EQCM) was developed by using an operational amplifier without any LC component. The home-made EQCM using this oscillator showed only 0.02 Hz frequency noise at 0.3 s gate time when a 6 MHz AT-cut crystal was used. Pb underpotential deposition on gold substrate in nitric acid media was examined to demonstrate the performance of this EQCM. The derivative of frequency change could be obtained without averaging multiple scans.

Introduction

Recently EQCM is being widely used as an *in situ* microgravimetric technique in electrochemistry to measure the changes of electrode mass concurrently with the electrochemical current and/or the electrode potential. Application of the *in situ* EQCM has been reviewed elsewhere.[1-3] Although the impedance measurement of the quartz crystal using an external impedance analyzer serves detailed information about each component of the impedance network,[4-8] the oscillator in which the quartz crystal is an active element is being commonly used for *in situ* microgravimetry or to monitor mass change continuously by simply measuring the frequency change.[9-21]

Various kinds of oscillator have been reported for the quartz crystal microbalance to be used in liquid system.[1,9,11,18,19,22-24] The oscillators based on transistor and LC tank circuit consist of some inductors and capacitors as well as some resistors.[18,22-24] The temperature coefficients of inductor(L) and capacitor(C) are relatively large compared with that of resistor(R) and the gain of transistor is not sufficiently high. To provide the necessary gain a two-stage transistor amplifier has been designed with many R, L, and C components.[18]

The use of integrated circuit (IC) makes the oscillator uncomplicated. Bruckenstein used transistor-transistor logic (TTL) ICs[9,19] for his EQCM study. In his circuit the electrode of quartz crystal that is also used as working electrode in electrochemical system was not grounded. Therefore, his circuit has to be isolated from the potentiostat to prevent flowing direct current (DC) by involving blocking capacitor or transformer. The different ground of oscillator from potentiostat can cause unexpected noise and careful attention has to be paid to stabilize the EQCM system.

Buttry used a video amplifier for the EQCM oscillator.[1,11] The advantage of Buttry's circuit is that the working electrode is grounded with both oscillator and potentiostat. Video amplifiers, however, are not quantitative compared with the operational amplifiers (Op. Amp.) which are more familiar with scientists. Furthermore this circuit requires LC components to be stabilized when a large mass is loaded on the quartz crystal.

*To whom correspondence should be addressed.

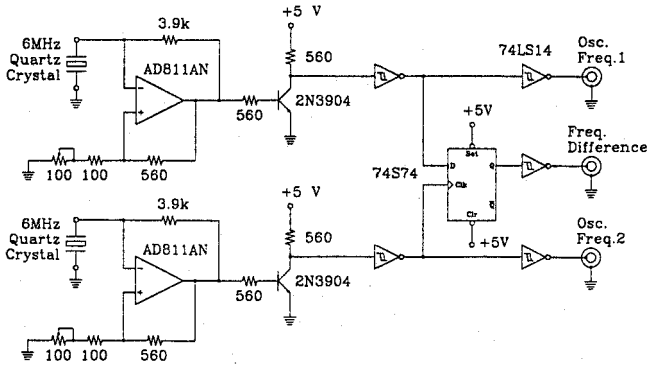

Figure 1. Block diagram of two oscillators and a frequency difference circuitry between these oscillators.

This contribution describes a new oscillator circuit for EQCM by introducing a wide band Op. Amp. without any LC component. This Op. Amp. circuit is very simple and the operation principle is easily understandable to the scientists. Further this circuit can be reproduced without expert knowledge on electronics.

Experimental

Circuit. As shown in Figure 1 the EQCM system consists of two oscillators and a frequency difference circuitry. One of these two oscillators was used for the reference quartz crystal and the other for the one to be tested. The frequency difference circuitry measures the instantaneous frequency difference between the two oscillators and output this difference. This configuration is advantageous to compensate the frequency drift due to the temperature change and/or to measure the frequency change precisely within the uncertainty of frequency counter.

Each oscillator was simply constructed using an Op. Amp. (AD811AN) and some resistors without any LC component. In this circuit the quartz crystal determines the negative feedback gain. At the resonance frequency the quartz crystal has the minimum value of its impedance. At this frequency the closed loop gain of the Op. Amp. according to the negative feedback goes larger than that of positive feedback and this circuit keeps oscillation. Positive feedback gain can be

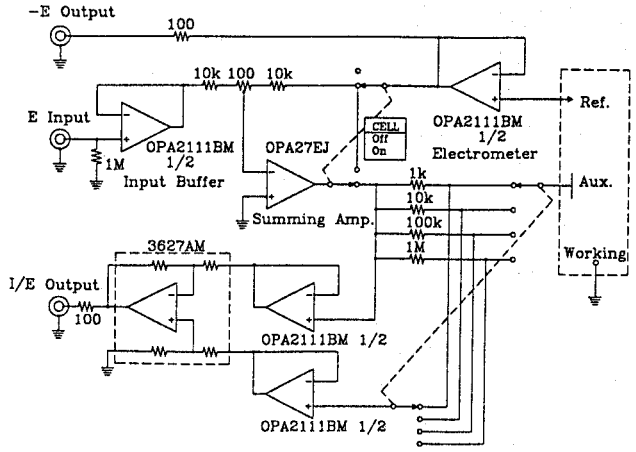

Figure 2. Circuit diagram of Wenking-style potentiostat.

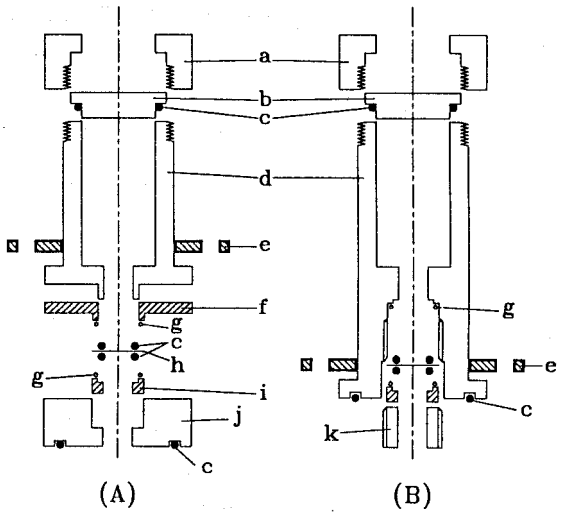

Figure 3. Cross sectional views of the cells used in this study. (A) Type-A cell, (B) Type-B cell. a, cell-top mount (polypropylene); b, cell top (Teflon); c, o-ring; d, cell body (Teflon); e, cell mounting ring (aluminum); f, contact plate (brass); g, contact spring (Cu-Be alloy); h, quartz crystal; I, crystal mount (brass); j, cell bottom (polypropylene); k, crystal mounting screw (PVC).

adjusted using 100 Ω variable resistor. Transistors (2N3904) were used to make analog signals compatible with subsequent TTL inputs. A simple frequency difference circuitry using a D-type flip-flop (74S74), that has been reported by Bruckenstein,[9] was introduced to get the frequency difference between two oscillators. The TTL 74LS14 (Hex Schmitt trigger inverter) served as input and output buffers.

Both two ±5 V power supplies for two oscillators and a +5 V power supply for TTL circuit were isolated by the use of individual voltage regulators to prevent any possible coupling or locking-in caused by the limited power supply rejection of Op. Amp. Each ground was connected to a ground plane.

One side of the crystal was grounded in the oscillator circuit and it was also used as a working electrode in a Wenking-type potentiostat as shown in Figure 2. OPA27EJ (Op. Amp.) served as a summing amplifier and an OPA2111 BM (dual Op. Amp.) was used for an electrometer and an input buffer. An instrumentation amplifier was composed of a differential amplifier (3627AM) with an OPA2111BM to measure the current flow through the precision resistor connected to the auxiliary electrode in series.

Cell. Two different type of electrochemical cells were designed. The cross sectional views of these cells are presented in Figure 3. Crystal (*h* in the figure) is mounted between two o-rings. It allows that the cell is watertight and the softness of o-rings can relieve the mounting stress of the crystal. Electrical connections to both sides of crystal were made with bent ring-shaped springs(*g*) made of Cu-Be (5%) wire. The springs under the crystal were soldered on the brass pieces(*i*). The spring above the crystal in type A cell was also soldered on the brass plate(*f*). External contact to the spring above the crystal in type B cell was made with a wire (not shown in the figure) inserted through a thin hole from the side of the main Teflon body. Type A cell was assembled by pressing down the cell mounting ring (*e*) against the aluminum block (not shown in the figure) using bolts. The assembly of type B cell was pressed against the ledge of the main Teflon body with a PVC screw(*k*). Two identical cells of each type were prepared for both reference and test cells.

A counter electrode made of gold wire and two Teflon tubes were housed through orifices drilled in the cell top(*b*) used for a test cell. One of two Teflon tubes was used to connect the solution inside to an external reference electrode (SCE) and the other was served only to maintain the internal pressure identical with the external pressure.

6 MHz AT-cut quartz crystals (Phelps Electronics Pe 102-03) were used in this study. The electrode in contact with solution is totally covered with gold and the opposite electrode is double-anchor shaped.

1 mM lead nitrate in 0.1 M nitric acid was prepared from 99.999% lead nitrate (Aldrich) and pro analysi nitric acid (Merck GR) which were used as received. Deionized water was doubly distilled in alkaline permanganate solution with a droplet trap for the preparation of solutions. Reference cell was filled with pure water.

Instrumentation. Electrode potential was programmed using the sweep generator of bipotentiostat (Pine AFRDE4). A Universal Counter (Hewlett Packard 53131A) was used to measure the frequency and a Measurement Plotting System(Hewlett Packard 7090A) served as a data acquisition system, both of which were connected to a personal computer *via* GPIB. Both reference and test cells were mounted on a common aluminum block that was placed on a vibration-free table (Dae Il Systems) with the EQCM. The connections between two cells and the EQCM were made as short as possible. All the experiments were performed at the ambient temperature of 25± 2 ℃.

Results and Discussion

Type A cell was originally designed to make both the electric connection and the crystal mounting easy. As shown in Figure 4, however, the frequency drift of type A cell was much larger than that of type B cell. Furthermore, compared with type B cell, much more time was required for type

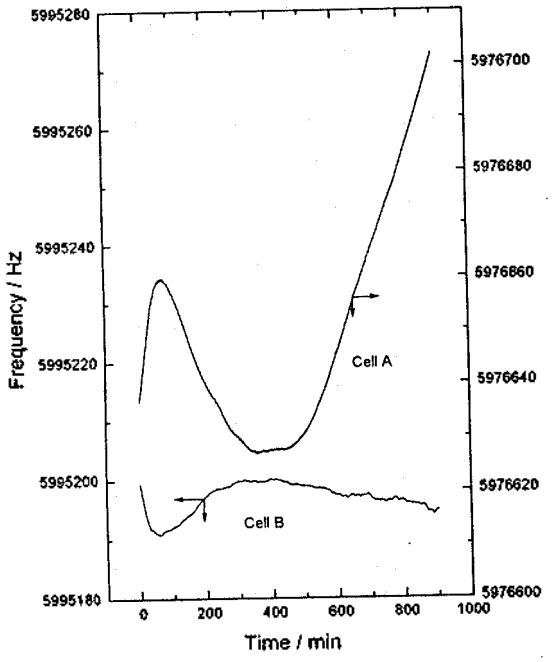

Figure 4. Frequency drifts of EQCMs using type-A or type-B cells filled with water. Frequency gating time, 1 s; sampling interval, 30 s.

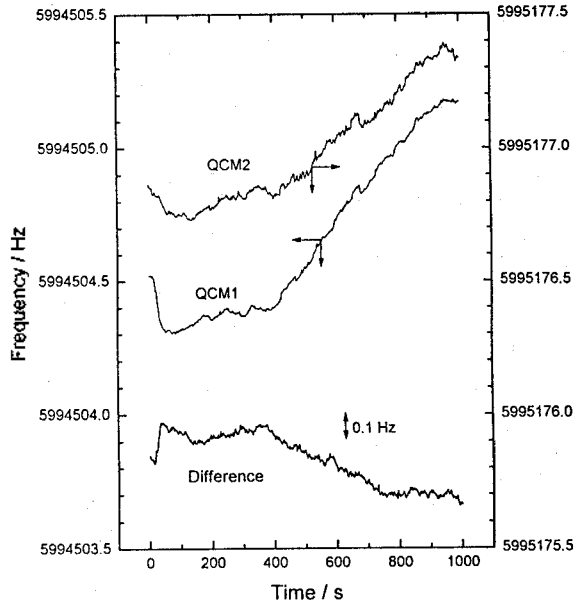

Figure 5. Frequency drifts of EQCM using type-B cells for both oscillators (QCM1 and QCM2). The frequency difference between QCM1 and QCM2 is also shown. Frequency gating time, 0.3 s; sampling interval, 1 s.

A cell to be stabilized. It is seemed to be associated with the temperature dependence of cell mounting stress. Type A cell has more pieces made of various materials than type B cell and it explains that the stress change of type A cell caused by the temperature change was more serious. If the stresses of the reference and test cells are same, the frequency difference between these two QCM has to be constant. In the case of type A cells the drifts of both reference and test cells could not show always same directions. Type B cells, however, have almost same trends of drift and Figure 5 shows the cancellation effect clearly. In this figure QCM1 and QCM2 mean the frequencies of both oscillators. The short term noise of the frequency difference was only 0.02 Hz at 0.3 s of gating time.

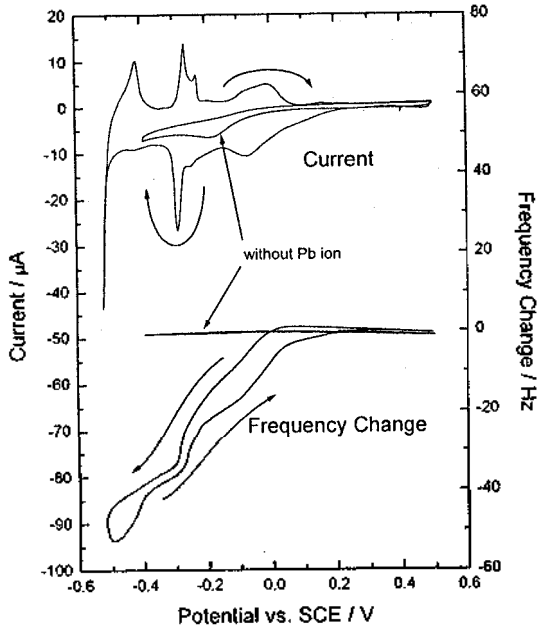

Figure 6. Current-potential and frequency-potential curves of EQCM in 0.1 M HNO_3 with and without 1 mM $Pb(NO_3)_2$. Scan rate, 10 mV/s; gate time, 0.1 s; sampling interval, 0.2 s.

Figure 6 shows performance of this EQCM system by involving a well-known monolayer process, the UPD of Pb on Au electrode. The solution was 1 mM lead nitrate in 0.1 M nitric acid. The curves were obtained after reaching steady state by continuous cycling of potential scan. The scan rate was 10 mV/s, the gating time of frequency counter was 0.1 s, and the sampling interval was 0.2 s. It is clearly shown that the frequency decreases during the Pb deposition and it increases while the reverse reaction occurs. The background current in the absence of Pb ion shows only reduction of dissolved oxygen molecules. Because this reaction does not cause the mass change of the electrode, there are only slight changes in frequency, which may be associated with the specific adsorption of electrolytes and water molecules. The negative limit is dictated by the reduction of hydrogen ions.

To compare the frequency change with the current, the first order derivative of the frequency data was obtained. Deakin and Melroy have averaged 20 scans to obtain a smooth derivative curve.[12] In this study, however, only one scan was sufficient to differentiate the frequency change. As shown in Figure 7, the current curve and the derivative curve of the frequency change have almost same shapes. The peaks *a* and *b* are corresponding to the UPD of lead monolayer on the gold substrate, and the peak *c* is associated with the bulk deposition of lead on the deposited lead layer in advance. Peak *d* is assigned to the stripping pair of peak

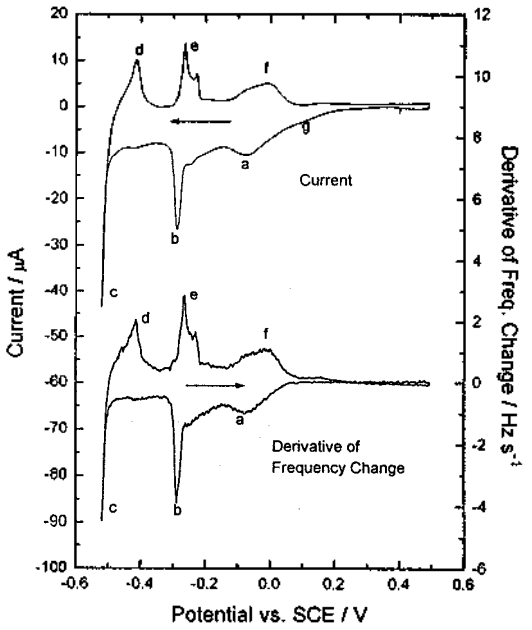

Figure 7. Current-potential curve and the first order derivative curve of frequency change. Data are from figure 6.

c, and the peaks *e* and *f* are the corresponding oxidation pairs of peaks *b* and *a*, respectively.

The broad shoulder *g* in the current-potential curve, however, has no corresponding part in the derivative curve of frequency change. It means that a reduction process occurs at that potential without mass change. If the lead ions present in the solution are reduced at the electrode surface, the electrode mass has to be increased. Based on the observation that there is no current in the background, it is believed that the lead ions had been adsorbed on the electrode surface at the anodic potential region and then were reduced at this potential. This phenomenon was not observed in perchloric acid media.[11,12] The catalytic reduction of nitrate or dissolved oxygen by the adsorbed lead species might be a possible cause for this prewave. Further works are being carried out to explain it explicitly.

References

1. Buttry, D. A. In *Electroanalytical Chemistry*; Bard, A. J., Ed.; Marcel Dekker: New York, U. S. A., 1991; Vol. 17, p 1.
2. Deakin, M. R.; Buttry, D. A. *Anal. Chem.* **1989**, *61*, 1147A.
3. Ward, M. D.; Buttry, D. A. *Science* **1990**, *249*, 1000.
4. Reed, C. E.; Kanazawa, K. K.; Kaufman, J. H. *J. Appl. Phys.* **1990**, *68*, 1993.
5. Martin, S. J.; Granstaff, V. E.; Frye, G. C. *Anal. Chem.* **1991**, *63*, 2272.
6. Lin, Z.; Yip, C. M.; Joseph, I. S.; Ward, M. D. *Anal. Chem.* **1993**, *65*, 1546.
7. Yang, M.; Thompson, M.; Duncan-Hewitt, W. C. *Langmuir* **1993**, *9*, 802.
8. Noël, M. A. M.; Topart, P. A. *Anal. Chem.* **1994**, *66*, 484.
9. Bruckenstein, S.; Shay, M. *Electrochim. Acta* **1985**, *30*, 1295.
10. Bruckenstein, S.; Shay, M. *J. Electroanal. Chem.* **1985**, *188*, 131.
11. Melroy, O.; Kanazawa, K.; Gordon II, J. G.; Buttry, D. A. *Langmuir* **1986**, *2*, 697.
12. Deakin, M. R.; Melroy, O. *J. Electroanal. Chem.* **1988**, *239*, 321.
13. Lakkaraju, S.; Bennahmias, M. J.; Borges, G. L.; Gordon II, J. G.; Lazaga, M.; Stone, B. M.; Ashley, K. *Appl. Optics* **1990**, *29*, 4943.
14. Gabrielli, C.; Keddam, M.; Torresi, R. *J. Electrochem. Soc.* **1991**, *138*, 2657.
15. Nivens, D. E.; Chambers, J. Q.; Anderson, T. R.; White, D. C. *Anal. Chem.* **1993**, *65*, 65.
16. Rivera, I. M.; Cabrera, C. R. *J. Electrochem. Soc.* **1993**, *140*, L36.
17. Lee, W.-W.; White, H. S.; Ward, M. D. *Anal. Chem.* **1993**, *65*, 3232.
18. Komplin, G. C.; Schleifer, F.; Pietro, W. J. *Rev. Sci. Instrum.* **1993**, *64*, 1530.
19. Bruckenstein, S.; Michalski, M.; Fensore, A.; Li, Z. *Anal. Chem.* **1994**, *66*, 1847.
20. Shana, Z. A.; Josse, F. *Anal. Chem.* **1994**, *66*, 1955.
21. Mo, Y.; Hwang, E.; Scherson, D. A. *Anal. Chem.* **1995**, *67*, 2415.
22. Nomura, T.; Okuhara, M. *Anal. Chim. Acta* **1982**, *142*, 281.
23. Bourkane, S.; Gabrielli, C.; Keddam, M. *Electrochim. Acta* **1989**, *34*, 1081.
24. Josse, F.; Shana, Z. A.; Radtke, D. E.; Haworth, D. T. *IEEE Trans. Ultras. Ferroel. Freq. Control* **1990**, *37*, 359.